

[15] Macromolecular Crystal Quality

By EDWARD H. SNELL, HENRY D. BELLAMY, and
GLORIA E. O. BORGSTAHL

“That which is striking and beautiful is not always good, but that which is good is always beautiful.”

Ninon De L’Enclos

Introduction

What is a good crystal? There are many criteria. Which we use depends on the qualities we seek. For gemstones, size, clarity, and impurity levels (color) are paramount. For the semiconductor industry, purity is probably the most important quality. For the structural crystallographer, the primary desideratum is the somewhat subtler concept of internal order. In this chapter, we discuss the effect of internal order (or the lack of it) on the crystal’s diffraction properties.

The internal order of a crystal can be characterized by a correlation length, i.e., the distance over which all the atoms in unit cells are “accurately” related by the crystal-symmetry operators (note that the unit-cell unit translational repeats are crystal symmetry operators). The importance of the correlation length in the context of X-ray diffraction is that an atom will contribute coherently to the intensity of a reflection only if its disorder relative to symmetry-related atoms is small compared to the resolution (d -spacing) of the reflection. Since the meaning of “accurately” depends on resolution, one can see that the correlation length, the accuracy of crystal repetitions, and the resolution of a reflection are all related. For a constant average random disorder in atomic position between adjacent unit cells, the disorder (symmetry-operator violation) between any two unit cells will increase as the square root of the distance between them. Therefore as resolution increases (d -spacing decreases) the effective correlation length decreases, and the number of unit cells contributing coherently to the diffraction decreases.

Random disorder is a major contributor to the reduction in diffracted intensity with increasing resolution. (In fact this is why the “temperature factor” has been renamed the “atomic displacement factor.”) Disorder can be described as long range or short range. In general long-range disorder in the crystal gives rise to localized effects in reciprocal space and vice versa.^{1,2} For example, crystal mosaicity, which is a large-scale property

in real space, causes the localized effect of broadened spots in reciprocal space. Random disorder between adjacent unit cells, a short-scale property in real space, is seen as a global, resolution-dependent reduction in diffracted intensity in reciprocal space. Thus, careful measurements of the diffraction from macromolecular crystals can reveal the degree and nature of their disorder. Since macromolecular crystals are, by the standard of small molecule crystals, not very good crystals, they offer a fruitful field for the study of disorder. It is our hope that a better understanding of the nature and causes of disorder in macromolecular crystals can lead to the production of better crystals.

Crystal Mosaicity and Domain Structure

The crystal properties that are amenable to investigation by reflection analysis are mosaicity and domain structure: mosaicity by profile analysis, and domain structure by topography and reciprocal-space mapping. The mosaic model of crystals was proposed by Darwin³ and approximates the crystal to an array of perfectly ordered volumes (domains) slightly misaligned with respect to each other. (The boundaries between these domains are ignored and no model for them is proposed.) We use this model as a first approximation to the real crystal since topographic evidence has revealed these domains,¹ and reasonably accurate calculations can be made from the model. In addition to having small random misalignments, the domains can be of varying volume and the unit cells in the crystal can vary (generally due to impurities). Each of these phenomena has a distinct effect on the crystal.^{1,2}

Figure 1 shows crystals as being made up of distinct domains according to the Darwin model and illustrates how physical features described by the mosaic model can be manifested in reciprocal-space mapping (center) and reflection-profile (rocking width) measurements (right side). The vectors q_{parallel} and $q_{\text{perpendicular}}$ in Fig. 1 (center) are parallel and perpendicular to the scattering vector, and are coincident with $\omega/2\theta$ and ω , respectively.^{4,5}

¹ T. J. Boggon *et al.*, *Acta Crystallogr. D* **56**(pt. 7), 868 (2000).

² C. Nave, *Acta Crystallogr. D* **54**(pt. 5), 848 (1998).

³ C. G. Darwin, *Philos. Mag.* **43**(257), 800 (1922).

⁴ V. Holy and P. Mikulik, in "X-Ray and Neutron Dynamical Diffraction: Theory and Applications" (A. Authier, S. Lagomarsino, and B. K. Tanner, eds.), p. 259. Plenum Press, New York, 1996.

⁵ P. F. Fewster, in "X-Ray and Neutron Dynamical Diffraction: Theory and Applications" (A. Authier, S. Lagomarsino, and B. K. Tanner, eds.), p. 269. Plenum Press, New York, 1996.

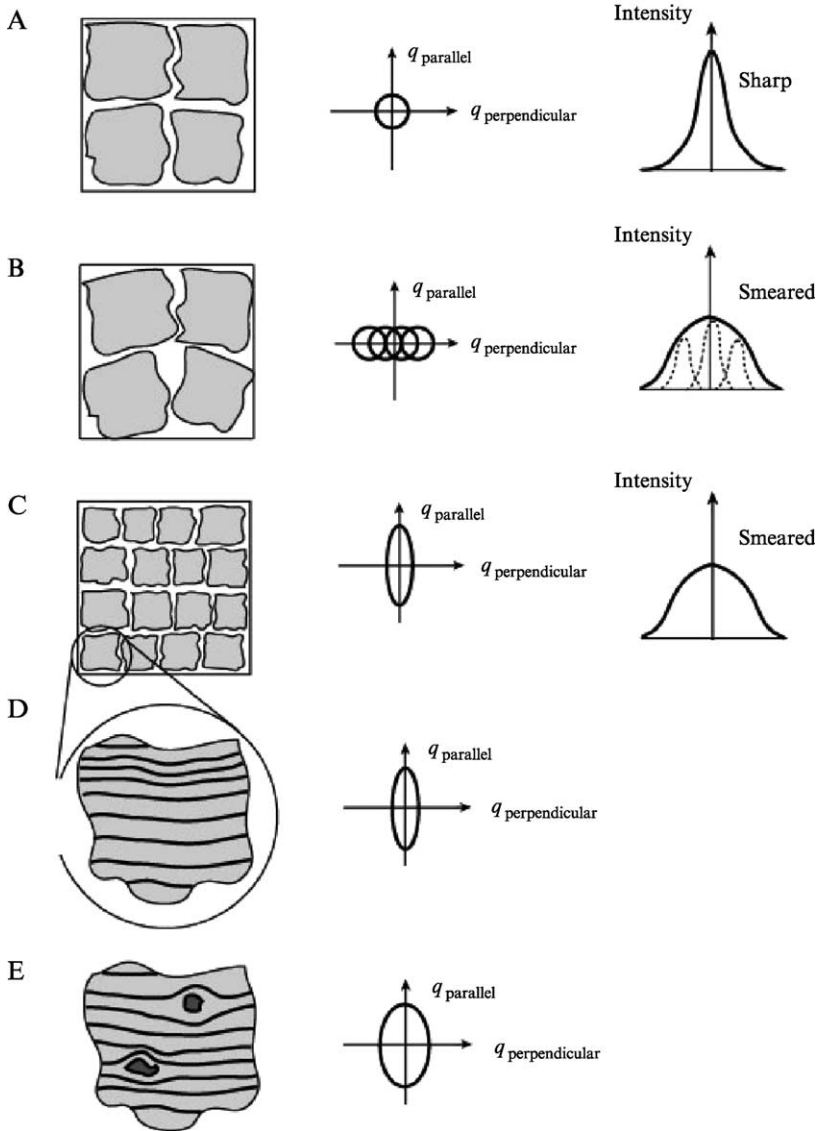


FIG. 1. Schematic diagram illustrating the influence of various physical properties of the crystal (left) on the reciprocal lattice point volume (shown in two dimensions center)¹ and the recorded reflection profile width (right). In (A) the crystal has a mosaic domain structure but the domains are well aligned. In (B) the domains are misaligned with respect to each other. This can be an anisotropic effect. Sharp reflections from each domain are distributed smearing out the overall profile. Well-aligned domains are shown in (C) with a reduced volume. This can be anisotropic but is resolution independent. Fourier truncation effects cause smearing

(Fig. 2A). Another way to think about it is that scans along q_{parallel} ($\omega/2\theta$) represent scans of d -spacing and scans along $q_{\text{perpendicular}}$ (ω) represent crystallite orientation. In the case shown in Fig. 1A all the domains are well aligned so their contributions to the reciprocal-lattice point overlap. Misalignment of the domains (Fig. 1B) broadens the reciprocal-lattice point along $q_{\text{perpendicular}}$ but causes no broadening along q_{parallel} . Figure 1C shows small, well-aligned domains. If the volume of the domains becomes very small the reflections will become broadened from Fourier truncation effects. That is, there aren't enough unit cells in the domain to give a sharp peak! When this is true, the reciprocal-lattice point is broadened in the q_{parallel} direction, and the effect is known as domain-size broadening.

A single domain, which is shown in Fig. 1D, has a lattice parameter variation that broadens the reciprocal-lattice point in the q_{parallel} direction. This lattice variation among unit cells causes a reflection to have slightly different Bragg angles, resulting in a smearing out of the reflection. Volume (domain-size) effects and lattice parameter variation (strain) can be distinguished only by making measurements at multiple resolutions. Volume effects are resolution independent, whereas lattice effects are resolution dependent. In a realistic case (Fig. 1E), point, line, and plane defects, volume, and misalignment all contribute to broaden the reciprocal-lattice point in both dimensions. All of the effects can be anisotropic. The analysis of individual reflections can provide a measure of the long-range order within the crystal. In addition, by making measurements in multiple regions of reciprocal space, crystal anisotropy can be investigated. Reflection analysis does not provide information about disordered loops and side chains, thermal vibrations, and other kinds of short-range disorder.

Experimental Methods

Crystal volume and physical appearance under the microscope give a qualitative description of crystal quality at best. The diffraction quality of a crystal is determined by features too small to be observed at optical wavelengths. Detailed analysis in reciprocal space provides a quantitative

out of the reflections from each domain when compared to larger domains. An enlargement of a single domain is shown in (D) with lattice variations and the reciprocal space map from a number of those domains illustrated. The effect can be anisotropic and is resolution dependent. Finally (E) shows a realistic case where a number of effects contribute. The effects of imperfections in the crystal are to smear the reflection intensity out and reduce the overall peak intensity.

measure. X-ray diffraction analysis techniques can be categorized into volume integrating, imaging, and three-dimensional profiling techniques.⁶ A unifying requirement in all three methods is that the properties of the incident X-ray beam should not mask the diffraction properties being measured. The relevant properties are vertical and horizontal divergence, wavelength bandwidth, and spatial uniformity of the beam.

In the traditional Ewald sphere construction, the sphere is an infinitesimally thin shell. This corresponds to a perfectly monochromatic beam with no angular divergence and the reflection width is governed by the mosaicity (Fig. 2A). A beam with nonzero beam divergence (Fig. 2B) and finite bandwidth (Fig. 2C) can be modeled by Ewald spheres with finite shell thicknesses. A perfect crystal would have extremely small, almost infinitesimal, reciprocal-lattice points. However, the mosaicity of a real crystal broadens the reciprocal lattice

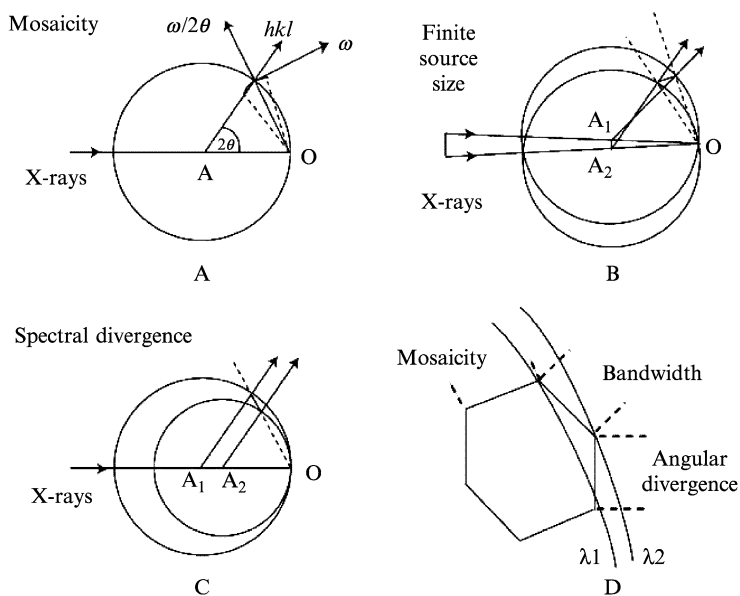


FIG. 2. An Ewald sphere illustration of broadening effects due to (A) crystal mosaicity, (B) angular divergence due to a finite source size, and (C) bandwidth. In (D) the region around the reciprocal lattice point is enlarged showing the combination of contributions. Dimensions have been exaggerated. Adapted from Aslanov *et al.*⁸ and Kheiker.

⁶ F. Otolora *et al.*, *J. Cryst. Growth* **196**, 546 (1999).

point can be totally encompassed in the thickness of the shell of the Ewald sphere, then the effect of the crystal quality on the reflection parameters will be masked and, in effect, only the beam parameters will be measured. When one investigates crystal quality, the probe, the X-ray beam, has to be configured carefully to prevent this. Typically in ordinary data collection the beam is focused to increase flux on the crystal. At synchrotron beamlines the bandwidth is not as narrow as it could be for the same reason.

An alternative approach is the Laue method, which uses polychromatic (“white”) incident radiation to illuminate a stationary crystal.⁷ The method is extremely sensitive to the mosaicity of crystals and simultaneously records a large number of reflections. Like the monochromatic method, Laue experiments require a highly parallel incident beam.

The Incident X-Ray Beam—Diffraction Geometry

The contribution of the vertical and horizontal angular divergence at the sample, γ_V and γ_H , respectively, and the bandwidth, $\delta\lambda/\lambda$, can be modeled in the Ewald construction. The beam divergence can be modeled by replacing the sphere with the locus of spheres resulting from a rotation of the nominal sphere around the origin of the reciprocal lattice, O , through γ_V and γ_H (Fig. 2B). The effect of finite bandwidth is modeled by two limiting spheres⁸ with radii $1/(\lambda - \Delta\lambda/2)$ and $1/(\lambda + \Delta\lambda/2)$ that are tangent to one another at the origin (Fig. 2C). An additional effect is that as the crystal is rotated, the reflections pass through the Ewald sphere with trajectories at differing angles of incidence to the surface of the sphere. This, of course, is the Lorentz effect and causes the angular width of the reflection to be increased independently of the quality of the crystal or the characteristics of the incident beam. Since we are not comparing the relative intensity of reflections the effects of polarization may be ignored.

For quantitative data processing, we must employ a number of equations that can be derived by an analysis of the Ewald construction. We summarize the most interesting of them here. Because a horizontal rotation axis is generally used at synchrotron beamlines we use H and V to denote directions along the rotation axis and perpendicular to both the rotation axis and the beam, respectively. The angular width for a reflection is given by^{9,10}

⁷ E. H. Snell *et al.*, *Acta Crystallogr. D* **51**, 1099 (1995).

⁸ L. A. Aslanov, G. V. Fetisov, and J. A. K. Howard, “Crystallographic Instrumentation.” IUCr Monographs on Crystallography. Oxford University Press, New York, 1998.

⁹ J. R. Helliwell, “Macromolecular Crystallography with Synchrotron Radiation.” Cambridge University Press, Cambridge, 1992.

¹⁰ H. D. Bellamy *et al.*, *Acta Crystallogr. D* **56**(pt. 8), 986 (2000).

$$|\phi_R| = \sqrt{L^2 \zeta^2 \gamma_H^2 + \gamma_V^2} + \frac{L\lambda}{d} \cos \theta_{hkl} \left[\eta + \left(\frac{\delta\lambda}{\lambda} \right) \tan \theta_{hkl} \right] \quad (1)$$

Here, ϕ_R is the measured reflection width, ζ is the position of the corresponding reciprocal lattice point projected onto the rotation axis, d is the resolution ($d = \lambda/2 \sin \theta_{hkl}$), η is the mosaic spread, and L is the correction for the Lorentz effect. If H and V are the horizontal and vertical distance of the observed reflection from the direct beam position then ζ^2 is given by

$$\zeta^2 = \left(\frac{H^2}{H^2 + V^2} \right) \sin^2(2\theta_{hkl}) \quad (2)$$

The Lorentz correction is given by

$$L = \frac{1}{\sqrt{\sin^2(2\theta_{hkl}) - \zeta^2}} \quad (3)$$

The reflection angle $2\theta_{hkl}$ is given by

$$2\theta_{hkl} = \tan^{-1} \left(\frac{\sqrt{H^2 + V^2}}{XTD} \right) \quad (4)$$

where XTD is the crystal to detector distance.

One can see that γ_V broadens the reflections universally over the detector, whereas the effect of γ_H on the reflection width depends on the position of the reflection on the detector and is maximum along the horizontal. The Lorentz effect is always maximal along the rotation axis, which in this case is horizontal. The wavelength dispersion term has its largest effect on high-resolution reflections. In Eq. (1) the correlated dispersion is ignored. Correlated dispersion is the variation of the wavelength across the beam, and is negligible with X-ray optics suitable for reflection analysis. Accurate structural and crystal-quality data collection has to overcome or correct for these contributions to the reflection profile in the integration process.

In the Laue case the mosaicity, η , is derived from the radial extension, Δ_{radial} , of the reflections:

$$\Delta_{\text{radial}} = 2\eta \frac{XTD}{\cos^2 2\theta} \quad (5)$$

This assumes an incident beam of zero divergence, and the relationship becomes more complicated if that criterion is not met. A large crystal-to-film distance (2.4 m was used in Snell *et al.*⁷) and a fine pixel-size detector, e.g., X-ray film, are required to make accurate measurements of Δ_{radial} .

The Incident X-Ray Beam—Practical Considerations

The ideal use of synchrotron radiation is in the unfocused case with a low bandpass monochromator. The method of multiple anomalous dispersion (MAD) also requires a highly monochromatic beam, and these beamlines, operated in unfocused modes, are ideal for investigating crystal quality. MAD beamlines use monochromators with $\delta\lambda/\lambda$ values on the order of 10^{-4} . Typical beamlines in normal operation, i.e., with a focusing mirror, have vertical divergences, on the order of 10^{-3} radians and horizontal divergences of several times that. The reflections will be broadened significantly [Eq. (1)] and the crystal properties will be completely masked.

An example of what could be achieved in terms of beam properties is provided by experiments performed at Stanford Synchrotron Radiation Laboratory (SSRL) beamline 1-5 (Fig. 3A). At the expense of X-ray intensity, the focusing mirror was dropped out of the direct-beam path in order to achieve values of 20 and 48 μ radians (about 0.001° and 0.003° , respectively) at the full width at half maximum (FWHM) for γ_V and γ_H , respectively. The bandwidth from the double crystal Si(111) monochromator is 2.4×10^{-4} and the correlated dispersion of the beam at the sample position is calculated to be 2.5×10^{-4} Å/mm (at 1.000 Å) in the vertical direction with no horizontal dispersion. The contribution of the instrument to the reflection profiles measured is a broadening of 0.0016° minimally. The broadening is least along the equatorial plane, i.e., perpendicular to the horizontal rotation axis. Recent alterations to beamline 1-5 currently prevent use of the unfocused beam for this type of experiment. Beamline 1-5 is a bending magnet beamline; an unfocused beam from an undulator source would be more intense with even less divergence.

Typical laboratory sources with focusing mirrors or graphite monochromators are not suitable instruments to study macromolecular crystal quality because of their high beam divergence. The home source can be configured for crystal quality measurements but only at the expense of X-ray intensity. For example, a Bartels type¹¹ monochromator can be used to condition the beam (Fig. 3A). This type of monochromator can achieve a geometric divergence of 52 μ radians and a spectral divergence of 1.5×10^{-4} using the Ge(220) reflection. Other optical systems, e.g., parabolic graded mirrors, can achieve reductions in the divergence characteristics¹² while increasing the available flux, but do not approach that available from the synchrotron.

¹¹ W. J. Bartels, *J. Vac. Sci. Technol. B* **1**(2), 338 (1983).

¹² H. M. Volz and R. J. Matyi, *Acta Crystallogr. D* **56**(pt. 7), 881 (2000).

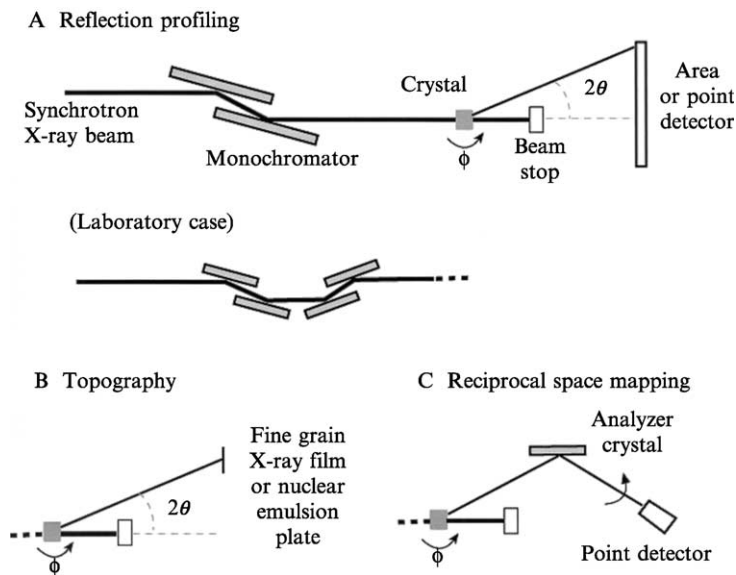


FIG. 3. Schematic diagram of the experimental setup to perform (A) reflection profiling (to obtain mosaicity) at the synchrotron using a double crystal monochromator, and in the laboratory with a Bartels monochromator, (B) topography using film/nuclear emulsion plates, and (C) reciprocal-space mapping showing the addition of an analyzer crystal. The Bartels monochromator in the laboratory setting (A) consists of two channel-cut crystals to condition the beam. In (C) the analyzer crystal and its associated point detector are moved together at a fixed $\theta/2\theta$ setting on a θ arm of the diffractometer.

Because of the inherently low intensity of the highly collimated and monochromatic X-rays from laboratory sources, and the weak scattering of macromolecular crystals, these sources are best used for the detailed study of reflections identified as containing useful information from previous synchrotron-based analysis. In this way, the synchrotron and the laboratory X-ray source can be used in a complementary fashion.

The methods used for crystal-quality measurements are reflection profiling, topography, and reciprocal space mapping. They have in common the requirement that the X-ray beam illuminates a reciprocal-space volume smaller than that of the reciprocal-lattice points being measured. The experimental setup for each is illustrated in Fig. 3. For reflection profiling (termed mosaicity analysis when the instrumental effects are deconvoluted out of the reflection profile due to the crystal), the instrumental setup is identical to standard modern structural data collection with the exception that an unfocused beam is used and the rotation angle between successive

images is very small, typically on the order of the instrument resolution function. For example, a ϕ step of 0.001° was used for the SSRL beamline 1-5 configuration described above, which had an instrument resolution¹³ of 0.0016° .

The Bartels monochromator consisting of two channel-cut crystals, each having its own $(n, -n)$ double reflection geometry is also illustrated (Fig. 3A). The first crystal produces a beam with a relatively large bandwidth but with a high correlation between the wavelength and beam direction. The second crystal is set such that the beam from the first crystal will strike it in dispersive geometry such that only a certain combination of wavelength and direction is passed out of the monochromator. Finally, the fourth reflection in the second crystal returns the now spectrally and geometrically collimated beam to its original direction. For topography (Fig. 3B) the area or point detector is replaced with a fine-grain film or a nuclear emulsion plate. Topography and reflection profiling can be accomplished using similar experimental setups. If the detector used for reflection profiling has sufficiently high spatial resolution, the topographs can be recorded simultaneously. Reciprocal space mapping is shown in (Fig. 3C). The analyzer crystal is made of the same material as the monochromator crystal(s). Both the analyzer crystal and the detector are carried on the 2θ arm.

Measuring the Quality of a Crystal

Mosaicity

We see from Eq. (1) that the width of a reflection profile, ϕ_R , is a function of the beam parameters, experimental geometry, and mosaicity. The angular extent of the reflection profile is termed the rocking width, generally evaluated as the FWHM of the rocking curve, ϕ_R . The mosaicity, η , is the contribution of the crystal to the measured rocking width. Thus mosaicity is the angular width of the reflection profile deconvoluted from beam, spectral, and Lorentz effects [Eq. (1)]. Mosaicity analysis measures the rocking width and deconvolutes the mosaicity from the other factors in the measured rocking width.

Shaikevitch and Kam¹⁴ published one of the first studies on the use of reflection profiling as an indicator of macromolecular crystal perfection. Subsequently Helliwell and co-workers made use of the synchrotron radiation properties described previously to minimize the geometric and

¹³ M. Colapietro *et al.*, *J. Appl. Crystallogr.* **25**, 192 (1992).

¹⁴ A. Shaikevitch and Z. Kam, *Acta Crystallogr. A* **37**, 871 (1981).

spectral contributions of the X-ray source to the experimental data.^{13,15}

The first measurements of mosaicity were made by recording reflections individually with a scintillation counter mounted in the equatorial (vertical) plane and by rotating the crystal about a horizontal axis.^{7,13,15–17} This experimental setup minimized the Lorentz effect and essentially eliminated the contribution from the horizontal divergence of the synchrotron beam [Eq. (1)]. Mosaicity analysis of chicken egg white lysozyme, apocrustacyanin C₁, and thaumatin crystals established a physical basis for the improvements seen in these microgravity-grown samples. The reduction in the mosaic spread in the microgravity-grown crystals produced a corresponding increase in the signal-to-noise ratio of the reflection. The minimum mosaicities recorded were 0.005° for lysozyme, 0.030° for apocrustacyanin C₁, and 0.018° for thaumatin.^{7,17,18}

Earlier methods^{1,7,13,16} looked at a few, low-resolution reflections recorded one at a time. The results, although intriguing, were not statistically robust owing to the paucity of data. We therefore developed a method using an area detector¹⁰ as did Ferrer and Roth.¹⁹ Our method combined superfine ϕ slicing data collection, unfocused monochromatic synchrotron radiation, and the use of a charge-coupled device (CCD) area detector in order to collect, index, and analyze hundreds of reflections in a short time.^{10,20} The crystal mosaicity, η , can be deconvoluted from the measured reflection width ϕ_R , by rearranging Eq. (1) above to^{10,20}

$$\eta = \frac{|\phi_R| - \sqrt{L^2 \zeta^2 \gamma_H^2 + \gamma_H^2}}{(L\lambda/d) \cos \theta_{hkl}} - \left(\frac{\delta\lambda}{\lambda} \right) \tan \theta_{hkl} \quad (6)$$

This method was first applied⁹ to crystals of *Escherichia coli* manganese superoxide dismutase (MnSOD).²¹ In one degree of data, the mosaicities of 260 reflections were measured. The mosaicity averaged 0.010° (SD 0.004°), measured as the FWHM, and ranged from 0.001° to 0.019°. Each reflection could be fitted with two Gaussian curves indicating that the crystal was composed of at least two mosaic domains. Indexing the reflections proved critical and allowed the anisotropic mosaicity to be related to the crystal packing based on the work of Ferrer and Roth.¹⁹ Another study on lysozyme²² developed a general expression:

¹⁵ J. R. Helliwell, *J. Cryst. Growth* **90**, 259 (1988).

¹⁶ R. Fourme *et al.*, *J. Synchrotron Radiat.* **2**, 136 (1995).

¹⁷ J. D. Ng, B. Lorber, R. Giegé, S. Koszelak, J. Day, A. Greenwood, and A. McPherson, *Acta Crystallogr. D* **53**, 724 (1997).

¹⁸ E. H. Snell *et al.*, *Acta Crystallogr. D* **53**, 231 (1997).

¹⁹ J.-L. Ferrer and M. Roth, *J. Appl. Crystallogr.* **33**, 433 (1998).

²⁰ J. Lovelace *et al.*, *J. Appl. Crystallogr.* **33**, 1187 (2000).

²¹ G. E. Borgstahl *et al.*, *J. Mol. Biol.* **296**(4), 951 (2000).

$$\eta_{hkl}^{\text{calc}} = \frac{\eta_{abc} \left[\frac{(ah)^2 + (bk)^2 + (cl)^2}{a^2 + b^2 + c^2} \right] + \eta_{def} \left[\frac{(dh)^2 + (ek)^2 + (fl)^2}{d^2 + e^2 + f^2} \right] + \eta_{mno} \left[\frac{(mh)^2 + (nk)^2 + (ol)^2}{m^2 + n^2 + o^2} \right]}{h^2 + k^2 + l^2} + \eta_{\text{const}} \quad (7)$$

where (a,b,c) , (d,e,f) , and (m,n,o) are real space vectors in the crystal lattice coordinate system, h,k , and l are the reflection indices, and η_{const} is the isotropic component of the mosaicity. Lysozyme proved to be isotropic in terms of mosaicity but this equation allows anisotropic mosaicity to be probed in terms of any defined direction, e.g., one related to the lattice or to the surface morphology.

Evaluating a statistically valid sample of indexed reflections becomes very important for comparative studies involving many crystals, for example, crystals grown by different methods, crystals of different morphologies, or for comparing crystal manipulations such as cryocooling protocols. As an example we describe a comparison of insulin crystals grown on earth with those grown in microgravity.²³ Using superfine ϕ sliced data, between 447 and 502 reflections were profiled for each of six microgravity-grown insulin crystals. Between 14 to 174 reflections were profiled for equivalently accumulated data from six earth-grown crystals (the earth crystals were much weaker diffractors so it was not possible to collect as many reflections from them). The crystals were not cryocooled. The best microgravity crystals had an average η of 0.002° with a standard deviation of only 0.001° —near the limit of resolution of the instrument configuration used. Two of the earth crystals had fairly low mosaicity with average η values of 0.013° (SD 0.004°) and 0.017° (SD 0.005°), respectively, yet these η values were 6.5 and 8.5 times higher than the best microgravity crystals and both crystals were relatively poor diffractors. For any given earth crystal, the η values for individual reflections varied over a surprisingly large range, with standard deviations of 0.004 to 0.024° . The spread in η for microgravity crystals was 4- to 5-fold narrower with standard deviations ranging from 0.001 to 0.005° . In a few cases, the best earth η values overlap the worst microgravity values. This illustrates the importance of collecting a statistically significant number of reflections from each sample since an unlucky selection of a few reflections could lead to an erroneous conclusion. A nonparametric, distribution-free, Mann–Whitney rank sum test confirms that the microgravity and the earth data are statistically different from each other at the 99% confidence interval.

²² E. H. Snell, R. A. Judge, L. Crawford, E. L. Forsythe, M. L. Pusey, M. Sportiello, P. Todd, H. Bellamy, J. Lovelace, Cassanto, and G. E. O. Borgstahl, *Cryst. Growth Des.* **1**(2), 151 (2001).

²³ G. E. O. Borgstahl *et al.*, *Acta Crystallogr. D* **57**, 1204 (2001).

It is important not only to collect a statistically significant number of reflections, but also to collect data from multiple samples: in this case six crystals of each kind. The microgravity crystals were on average 34 times larger, had 7 times lower mosaicity, had 54 times higher reflection peak heights, and diffracted to significantly higher resolution than their earth-grown counterparts. Figure 4 shows an example of a reflection profile for one of the earth-grown crystals decomposed into three Gaussians. Figure 5 illustrates the effect of reduced mosaicity on the quality of the data obtained from examples of the insulin crystals in the study described. Crystals with reduced mosaicity produced data with a higher signal-to-noise ratio. The mosaicity of a crystal is not directly related to diffraction resolution, but crystals of lower mosaicity produce a higher peak intensity that may be detectable at higher resolution.

During structural data collection the correct ϕ step can take advantage of reduced mosaicity to maximize the signal-to-noise ratio, thereby improving the useful resolution in the data.²⁴ Reduced mosaicity increases the number of fully recorded reflections per image and reduces spatial

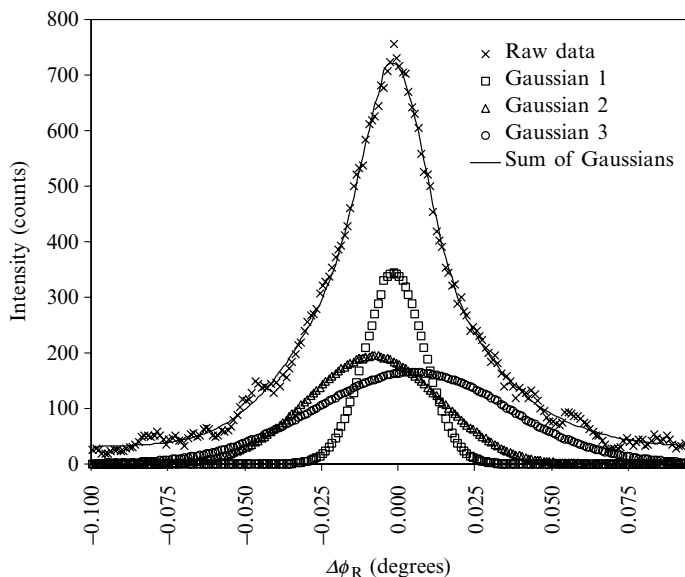


FIG. 4. Profile of the $(5 - 16 3)$ reflection from an earth-grown insulin crystal.²³ This reflection was accurately fitted by the sum of three Gaussians. The measured FWHM, ϕ_R , was 0.036° with a mosaicity, η , after suitable deconvolution of 0.010° .

²⁴ J. W. Pflugrath, *Acta Crystallogr. D* **55**, 1718 (1999).

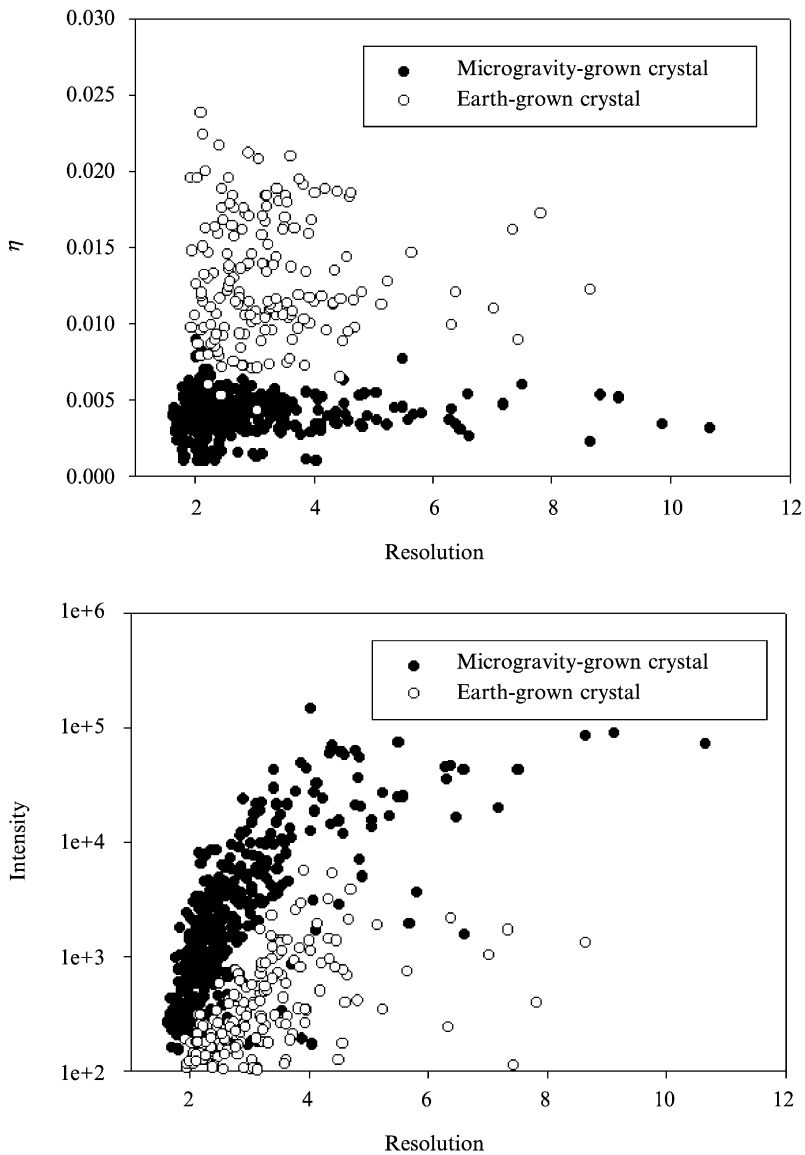


FIG. 5. Crystal quality comparison of insulin crystals used in a microgravity versus ground-growth study. Mosaicity and background-subtracted intensity are plotted against resolution. The data were cut off at the detector edge. Maximum intensity normalized to a 2 sec exposure is plotted on a log scale. Resolution is in Å and η in degrees. Further details can be found in Borgstahl *et al.*²³

overlap.²⁵ Fine-sliced images using oscillation methods can be used to take advantage of low mosaicity, but the method does present technical difficulties. The data may suffer from increased detector readout noise, and the shorter, narrower images place more stringent requirements on the hardware for shutter timing and goniometer control.²⁴ The time lost during detector readout is also increased. In studying mosaicity, superfine ϕ slicing provides the necessary detail. However, for structural data collection where the beam is not as parallel and possibly not as monochromatic, there is little or nothing to be gained with oscillations less than one-third to one-half of the greater of the beam contribution or the crystal mosaicity.²⁴ It is important, of course, to understand the characteristics of the beamline before starting, and to process the data as they are collected to maximize their quality.

Topography

X-ray topography is an imaging technique that is essentially the visualization of individual reflections: images of the diffracting parts of the crystal at a particular, stationary, orientation. It is the study of ways that irregularities in the lattice cause locally changing diffracted intensities (contrast) within individual reflections.¹ Topographs are a measure of the scattering power of a crystal as a function of position across the diffracted X-ray beam. In most cases, it is not the defect itself but the variations in the lattice surrounding the defect that produce the contrast. Intensity variations are related to the type and volume distribution of defects. Three causes of contrast are orientation variations owing to domain misalignment, extinction caused by a high strain gradient, and dynamic scattering effects. The last is small for weakly scattering macromolecules. A high-quality region of the crystal will have a uniform dark or light area in the topograph. The maximum spatial resolution obtainable in a topograph is about 2–3 μm with photographic film and 1 μm with nuclear-emulsion plates.

Topography on macromolecular crystals was suggested by Shaikevitch and Kam.¹⁴ Stojanoff and Siddons²⁶ used the white Laue beam to study lysozyme crystals. Highly strained regions, high densities of defects, and quite perfect regions were seen. The topographs were surprisingly detailed. Fourme *et al.*¹⁶ used reflection profiles to take topographs at different Bragg angles of multiple peaks seen in the same reflection, again from lysozyme. They discovered separate regions or domains of the crystal contributing to each peak of the total reflection.

²⁵ R. Fourme *et al.*, *J. Cryst. Growth* **196**, 535 (1999).

²⁶ V. Stojanoff and D. P. Siddons, *Acta Crystallogr. A* **52**, 498 (1996).

Topography has been used as an effective technique to study the effect of solution variations during crystal growth.²⁷ Topographs of lysozyme crystals subjected to deliberate variation of temperature, pH, or mother liquor concentrations during their growth revealed several general effects. Lysozyme is relatively insensitive to changes in growth conditions compared to most macromolecules, so the changes employed were large. Temperature was changed from 295 to 288 K, pH from 4 to 5, and in combination protein concentration reduced from 65 to 11 mg ml⁻¹ while salt was increased from 0.45 to 1.2 M. The authors also studied the effects of protein concentration by transferring growing crystals from a 27 to a 41 mg ml⁻¹ protein concentration solution. This increase in protein concentration mimics a seeding experiment. In crystals subjected to a pH change, the scattered intensity from the boundary layer just outside the prechange region differs strongly from both earlier and subsequent regions. The lattice growing during the change is more disordered than that before and that shortly after. It seems that crystal perfection recovers in subsequent lattice growth. A similar effect is seen for concentration changes of both the protein and salt. Temperature change causes a difference in the mosaicity or lattice dimensions. A factor of three increase in the growth rate did not produce substantial features in the resulting topographs. This suggests that during the growth process, a change of protein concentration in the drop will not necessarily affect the quality of the resulting crystal. By application of reflection profiling in the same experiment it was concluded that the contrast variation seen in the topograph is primarily due to lattice mosaicity (Fig. 1B).

Topographs acquired at successive angles within the reflection profile will map out the contribution of the crystal to each point of that profile. Figure 6 illustrates topographs from two high quality lysozyme crystals. In Fig. 6a and b the crystal clearly consists of two major domains whereas the crystal illustrated in Fig. 6c and d consists of several domains separated by boundary areas.¹ With an undulator source the angular divergence of the beam can be very small and the spatial resolution in the topograph high. The different growth sectors within the crystal can be imaged, and, more remarkably, fringes at the boundaries of those growth sectors can be seen.⁴ Topography provides a strong but qualitative method suited to the study of crystal growth and other practical applications such as the study of cryoprotectant effects on cooling.²⁸

²⁷ I. Dobrianov *et al.*, *Acta Crystallogr. D* **54**, 922 (1998).

²⁸ S. Kriminski *et al.*, *Acta Crystallogr. D* **58**, 459 (2002).

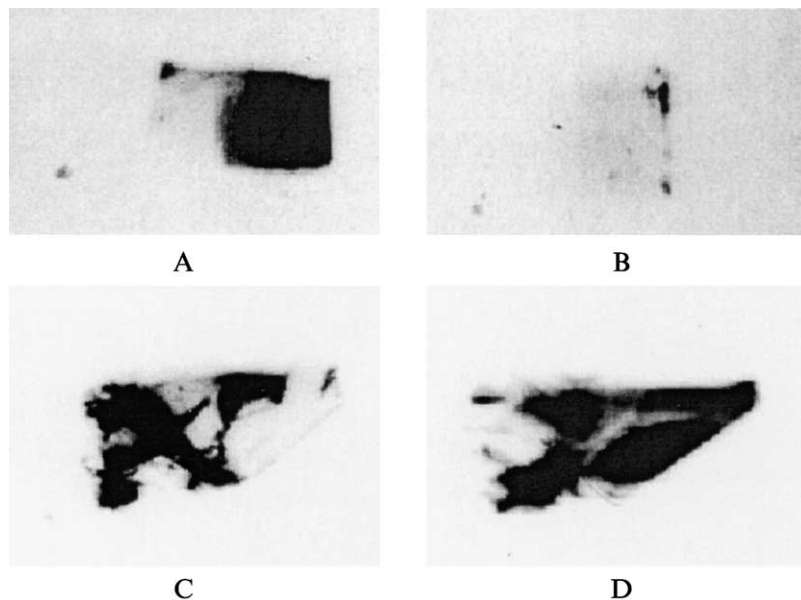


FIG. 6. Topographs taken from two high-quality lysozyme crystals.¹ Each topograph is a greatly magnified image of a single reflection. In (A) and (B) the crystal is 1.1 mm by 0.9 mm in projection, and defined regions are seen at the different reflections of (A) and (B). Some scattering is also seen on the crystal edges, probably due to mounting. In (C) and (D) the crystal is 1.5 mm by 1.1 mm in projection. In this case an array of domains is seen separated by a boundary layer. The different reflections (C) and (D) illustrate a region in the lower right of the crystal coming into the Bragg diffracting condition at the current ϕ orientation. The properties of the monochromatic beam are well illustrated in this case showing the clearly defined shape of the crystal rather than any collimation or divergence properties.

Reciprocal-Space Mapping

Although the term reciprocal-space mapping can be used to describe all methods of diffraction data collection²⁹ we use it in a more limited sense to describe examining a volume of reciprocal space around each individual reflection in two or three dimensions. Both reflection profiling and topography image the reciprocal lattice over a relatively large volume causing much information about the shape of the reciprocal-lattice point to be lost. Reciprocal-space mapping provides the shape information lost from the other techniques. The effects shown in Fig. 1 contribute to the measured mosaicity. Reciprocal space mapping allows us to understand mosaicity in terms of the components that contribute to it.

²⁹ P. F. Fewster, *Crit. Rev. Solid State Mater. Sci.* **22**(2), 69 (1997).

Reciprocal-space mapping is accomplished by a sampling of the reflection profile using an analyzer crystal in the path of the diffracted beam (Fig. 3C). The reciprocal-space map is recorded by mapping in both the sample crystal and the detector angles. The direction of these scans is illustrated in Fig. 2 where ω translates to q_{parallel} and $\omega/2\theta$ to $q_{\text{perpendicular}}$ of Fig. 1. Reciprocal-space mapping is a high-fidelity technique, but because it is time consuming only a few reflections can be studied from one sample. Therefore the most effective study would combine reciprocal-space mapping with one or more other techniques.¹ For example, one would identify reflections of interest by area-detector mosaicity analysis, and then these selected reflections could be studied in detail by reciprocal-space mapping. Reciprocal-space mapping of macromolecular crystals was first performed in the laboratory using a Bartels monochromator system. Lysozyme was extremely weakly scattering but produced very sharp profiles.²⁹ Later, experiments with synchrotron radiation produced similar results (Fig. 7).¹ By recording maps at multiple χ positions, a rotation parallel to the beam, a three-dimensional profile of the reciprocal lattice can be built up.²⁹

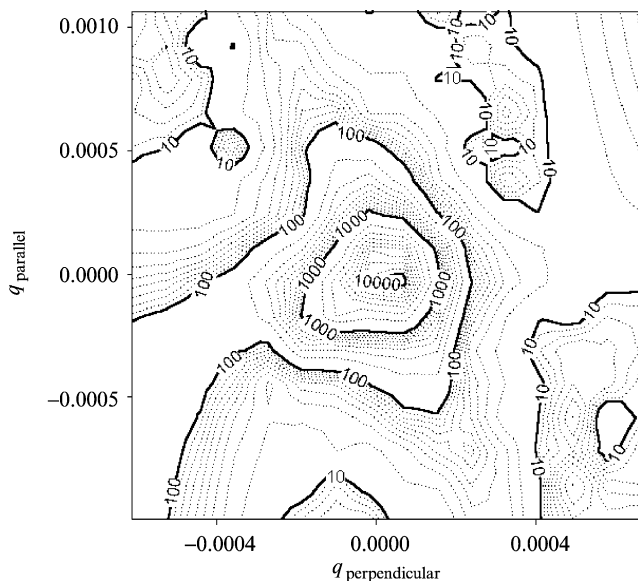


FIG. 7. Example of a reciprocal-space map of reflection (13 1 8) from a lysozyme crystal of $0.7 \times 0.7 \times 0.4$ mm in dimension. The mosaicity for this sample was 0.002° with q_{parallel} of 1.0×10^{-4} and $q_{\text{perpendicular}}$ of 0.9×10^{-4} at full width at half height maximum. The units of q are $2\pi/\lambda$ with λ being 1.0 Å in this case. Further details can be found in Boggen *et al.*¹

Lysozyme crystals were found to present a complex analysis problem since reciprocal-space mapping data reveal that they appear to lie at the convergence of the kinematic (ideally imperfect crystal model) and dynamic (ideally perfect crystal model) treatments of diffraction.¹² Kinematic diffraction ignores the interaction of wave fields within the crystal and is valid for a crystal that is small compared to the extinction distance ε defined by³⁰;

$$\varepsilon = V_c / (r_0 C |F_h| \lambda) \quad (8)$$

where C is the polarization factor, V_c the volume of the unit cell, r_0 the classic electron radius, $|F_h|$ the amplitude of the structure factor, and λ the wavelength. Dynamic theory allows the coupling of the wave fields within the crystal and accounts for extinction effects. For X-ray wavelengths and macromolecular crystals, the extinction distance has been reported to be on the order of a millimeter.^{12,15,16} The mosaicity can be predicted from both kinematic and dynamic theory. The values predicted from both theories turn out to be similar.¹² Dynamic theory can have an important impact for structural crystallography on the accuracy of the integrated intensities, especially of the lower resolution, more intense reflections. Polykarpov and Sawyer³¹ derived an extinction correction that takes into account dynamic properties in macromolecular crystals. They found that in the case of alcohol dehydrogenase the correction may be as much as 15% for the strongest, low-resolution reflections, and that as many as 20% of all the reflections at a resolution lower than 3.4 Å had to be corrected by more than 2% compared to kinematic diffraction data.

The considerable length of time required for reciprocal-space mapping makes radiation damage a concern. Fortunately, when unfocused, highly monochromatic radiation is used, samples receive far lower doses than for an equivalent time of structural data collection. Radiation damage is both time and dose dependent but Voltz and Matyi³² report a case of 5 days of continuous radiation not affecting data from a lysozyme sample on a well-conditioned laboratory beam.

Reciprocal-space mapping reveals information that cannot be seen through measurement of mosaicity or topography. The technique has been used with great success in the semiconductor industry owing to a

³⁰ D. K. Bowen and B. K. Tanner, "High Resolution X-ray Diffractometry and Topography." Taylor & Francis, Bristol, PA, 1998.

³¹ I. Polykarpov and L. Sawyer, Correction on perfection: Primary extinction correction in protein crystallography. Joint CCP4 + ESF-EAMCB. *Newslett. Protein Crystallogr.* **31**, 5 (1995).

³² H. M. Volz and R. J. Matyi, *J. Cryst. Growth* **232**, 502 (2001).

comprehensive practical and theoretical understanding of the sample material.²⁹ Macromolecular crystals are far more complex systems, and theory has yet to catch up with experiment in understanding just how much information reciprocal-space mapping can reveal in the macromolecular world. It is one of the developing areas in crystal quality analysis.

The Complete Picture

Mosaicity, topography, and reciprocal-space mapping are all techniques to probe the physical characteristics of the crystals through their interaction with X-rays. The techniques described are complementary. For example Boggon *et al.*¹ combined the three techniques with synchrotron radiation in the study of microgravity and ground grown crystals. Only a small number of samples were used, but microgravity crystals showed a reduced mosaicity. Reciprocal-space maps saw no change in stress, and topography showed that the majority of the crystal was contributing to the peak of the reflection at the appropriate Bragg angle in the microgravity case. Each technique provided unique information, and each technique also provided complementary information.

In terms of structural crystallography, i.e., solving and understanding the structure of a macromolecule of interest, having a high-quality crystal is clearly desirable. The techniques described here are not part of routine data collection. Of the techniques described, mosaicity measurements can be performed relatively easily and are the most useful in the short term. The quality of the data can be optimized by matching the oscillation range to the mosaicity. The background in an oscillation image builds up throughout the oscillation range but the reflection is recorded over only a finite angle. In the future “ideal” data collection may be possible by continuous rotation with real-time detector readout offering effectively infinitely fine slicing.

Mosaicity, topography, and reciprocal-space mapping are diagnostic techniques that allow us to ask questions about the practical effects of the crystal growth process and the data collection practices in order to optimize them. They offer quantitative data about crystal growth methods, biochemical properties, and practical matters such as cryocooling protocols, cryogens, and crystal handling for automated studies. The resolution of the structural data and corresponding electron density maps provide us with an indication of the short-range quality. The techniques described here give us a measure of long-range order. Many of the crystal-quality techniques have been developed with lysozyme; the future will see them being applied to more real-life cases. Eventually crystal growth, now an empirical process of rational trial and error guided by past experience,

may be understood in far greater detail with information from reflection analysis. A surprise has been just how ordered macromolecular crystals can be. This offers potential in new phasing methods such as multiple beam diffraction³³ and the exploitation of the coherent radiation opportunities available at third-generation synchrotron sources.

Acknowledgments

We thank Drs. Jeff Lovelace and Ardeschir Vahedi-Faridi (Toledo), Titus Boggon (New York), Peter Siddons (Brookhaven), and Prof. John Helliwell (Manchester) for technical and scientific contributions. This work was funded by NASA Grants NAG8-1380, NAG8-1825, and NAG-1836. E.H.S. is contracted to NASA through BAE-SYSTEMS Analytical Solutions.

³³ E. Weckert and K. Hummer, *Acta Crystallogr. A* **53**, 108 (1997).

[16] Protein Structures at Atomic Resolution

By ZBIGNIEW DAUTER

Introduction

In recent years there has been a dramatic increase in the number of X-ray crystal structures of proteins refined at atomic resolution. This trend has been anticipated¹⁻³ and exceeds even the growth of the number of all protein structures deposited at the Protein Data Bank (PDB) (Fig. 1). There is no doubt that this explosion of atomic resolution structures is owed mainly to the advances in macromolecular crystallography methodology. The most important advances have been in the practice of crystal growth. The availability of convenient and quick protein-purification methods, efficient crystal-growth screening conditions, convenient crystallization chambers that employ only small amounts of sample, and sometimes mechanisms (robots) to automate the setting up of crystallization trials all contribute to these successes. A number of atomic resolution data have been obtained from crystals grown in microgravity, which makes it possible to use efficiently the full diffraction potential of very-high-quality protein crystals. The availability of bright synchrotron beam lines,

¹ Z. Dauter, V. S. Lamzin, and K. S. Wilson, *Curr. Opin. Struct. Biol.* **3**, 784 (1995).

² Z. Dauter, V. S. Lamzin, and K. S. Wilson, *Curr. Opin. Struct. Biol.* **7**, 681 (1997).

³ S. Longhi, M. Czjzek, and C. Cambillau, *Curr. Opin. Struct. Biol.* **8**, 730 (1998).